Nuclear Instruments and Methods in Physics Research B55 (1991) 615–619
North-Holland

Channeling implantation of B and P in silicon

R.J. Schreutelkamp, V. Raineri [1] and F.W. Saris
FOM Institute for Atomic and Molecular Physics, Kruislaan 407, 1098 SJ Amsterdam, The Netherlands

R.E. Kaim, J.F.M. Westendorp [2] and P.F.H.M. van der Meulen
Varian/Extrion Division, 123 Brimbal Avenue, Beverly, MA 01915, USA

K.T.F. Janssen
Philips Research Laboratories, P.O. Box 80000, 5600 JA Eindhoven, The Netherlands

Highly uniform profiles of B and P ions have been obtained by channeling implantations in 150 mm diameter Si(100) wafers. Large differences in penetration depth, doping depth profiles and implantation damage are observed between implantations under channeling and random conditions for a wide range of doses and ion energies using Rutherford backscattering spectrometry, cross-sectional transmission electron microscopy and secondary-ion mass spectrometry.

1. Introduction

Channeling implantation offers several advantages over conventional ion implantation [1]. When the ion beam is aligned along one of the major axes of a crystal less damage is created and the penetration depth of the ions is considerably larger. However, applying the channeling technique requires a high degree of uniformity which has prevented the use of channeling implantation in conventional ion implanters. Recently a new ion implanter, the Varian 220, has been introduced which has the potential to successfully perform channeling implantation on wafers as large as 200 mm. The beam is scanned by means of a combined electrostatic/mechanical scan system [2]. In the horizontal direction the beam is scanned electrostatically; a parallel scan is achieved by means of a nonuniform dipole magnet [3]. The wafer is mechanically translated vertically [4]. The application of this parallel beam scan has already been shown to be useful for the formation of high-quality trench sidewalls for VLSI manufacturing [5].

In this paper we present an overview of doping depth profiles obtained by channeling implantations of B^+ and P^+ ions in 150 mm silicon wafers for various energies and doses. A comparison is made between channeled and random conditions. Furthermore, the differences in damage both before and after thermal annealing are investigated.

2. Experimental

Implantations were performed with a Varian/Extrion 220 medium-current ion implanter at Varian/Extrion [2]. Boron was implanted in 1–2 Ω cm, n-type Czochralski-grown 150 mm silicon wafers of (001) substrate orientation along channeling and random directions at energies ranging from 5 to 380 keV and doses from 1×10^{12} to 2×10^{15} cm^{-2}. Phosphorus implantations were done in 1 Ω cm, p-type Czochralskri-grown silicon wafers at an energy of 100 keV and doses between 1×10^{13} and 1×10^{15} cm^{-2}. The channeling implantations were done along [001], while the random direction corresponded to a tilt of 10° off normal and a twist of 15° with respect to the flat positioned horizontally.

Rapid thermal annealing (RTA) was done in an AG Associates Heatpulse 410 rapid thermal processor under a continuous Ar flow. Conventional anneals were done in a vacuum furnace with a base pressure $< 10^{-7}$ Torr. Secondary-ion mass spectrometry (SIMS) analysis was used to determine the boron and phosphorus profiles. The SIMS measurements were carried out with a Cameca IMS 3f or 4f instrument. For P-implanted samples a 14.5 keV Cs^+ primary beam was used. The 5 and 10 keV B profiles were measured using a primary beam of 3.0 keV, 0.25 μA O_2^+ in an oxygen ambient in

[1] Permanent address: University of Catania, Corso Italia 57, 95100 Catania, Italy.
[2] Permanent address: ASM International, P.O. Box 100, 3720 AC Bilthoven, The Netherlands.

0168-583X/91/$03.50

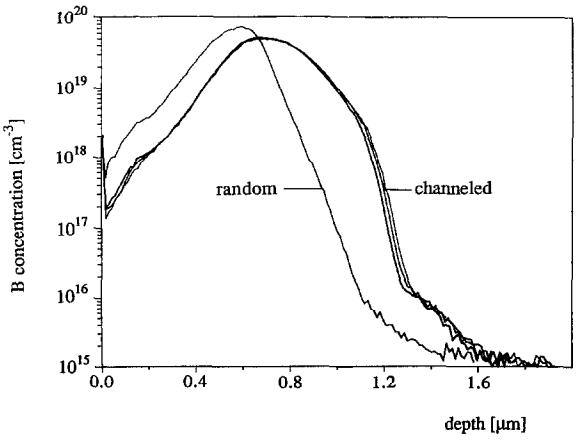

Fig. 1. Doping profiles measured with SIMS for 200 keV B^+ 2×10^{15} cm^{-2} channeling and random implantations. For the channeling implantation profiles are shown from two spots on opposite sides of a 150 mm wafer and at one spot in the center.

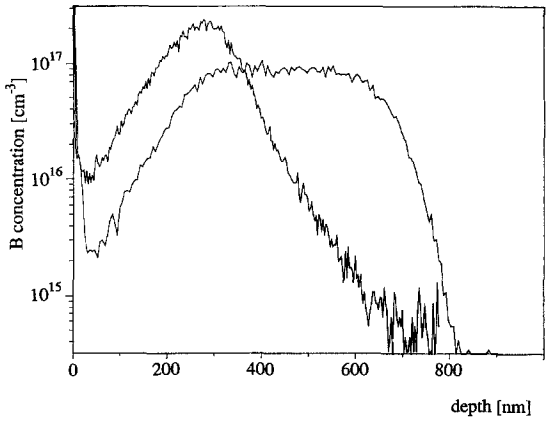

Fig. 3. Boron depth profiles for 80 keV 4×10^{12} cm^{-2} implantations under channeling and random conditions are compared.

order to resolve the near-surface part of the profile ($p(O_2) = 2\times10^{-5}$ Torr). For higher-energy B-implanted samples a primary beam of 6.5 keV, 0.7 μA O_2^+ was used. The scanned area was 250×250 μm^2 and the diameter of the analyzed area was $\varnothing = 60$ μm.

3. Results

3.1. Boron implantations in Si(100)

Fig. 1 compares the doping profiles of 200 keV 2×10^{15} cm^{-2} ^{11}B ions implanted in Si(100) under channeling and random conditions. The three channeled doping profiles shown were measured at three different spots across a 150 mm Si wafer along a line parallel to the horizontal electrostatic scan. One spot was in the center, while the other two spots were at opposite sides of the wafer. The maximum penetration depth of the channeling implantations was $R_{max} = 1.23$ μm, in excellent agreement with the calculated value of $R_{max} = 1.22$ μm based on the modified Firsov theory [6]. The maximum penetration depth is defined as the depth required to stop all but 1% of the particles [7]. The critical angle for channeling of 200 keV B ions is ≈ 2°; earlier, we have found that an angular variation of 1° has a significant influence on the resulting doping depth profile [8]. Since we do not observe a difference in the B profile at the three spots this means that well channeled conditions were maintained across the wafer. The uniformity has also been checked for various ion species, implantation energies and doses using sheet-resistance measurements and RBS [9,10]. For all channeling implants we found the peak of the doping depth profiles to be uniform within 1%.

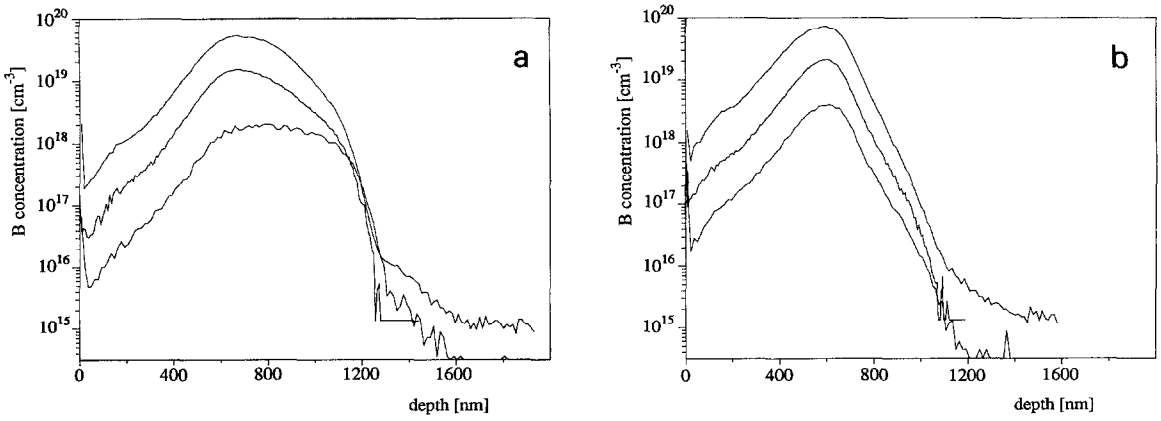

Fig. 2. Boron profiles for 200 keV implantations at doses of 1×10^{14}, 5×10^{14} and 2×10^{15} cm^{-2} under channeling (a) and random (b) conditions.

Fig. 2 shows the doping depth distributions for several 200 keV ^{11}B doses under channeling and random conditions. The doses shown are 1×10^{14}, 5×10^{14} and 2×10^{15} cm^{-2}. Implantation of 1×10^{14} cm^{-2} under channeling condition results in a constant doping level of 2×10^{18} cm^{-3}. The depth doping profiles obtained after the implantations of 5×10^{14} cm^2 and 2×10^{15} cm^{-2} are peaked at 0.69 μm, close to the projected range $R_p = 0.59$ μm for implantation under random condition. These results show that the difference between channeling and random implantations is no longer pronounced above a dose of 1×10^{14} cm^{-2} owing to dechanneling from the buildup of disorder as the dose is increased.

In fig. 3 the depth profiles for channeled and random implants of 80 keV 4×10^{12} cm^{-2} B^+ ions are compared. A nearly Gaussian profile peaked at 0.28 μm results after a random implant in good agreement with the projected range calculated by TRIM [11] of 0.26 μm. We observe that the B profile has a tail at the substrate side of the wafer apparently caused by channeling effects in crystalline Si, as was pointed out by Hofker et al. [12]. A flat doping depth profile results for the channeled implantation. The B concentration beyond the maximum penetration depth falls off at 21(2) decades/μm, much sharper than for the random implants. The maximum B penetration depth of 0.74 μm is in excellent agreement with the calculated value of 0.77 μm based on the modified Firsov theory [6].

Fig. 4 shows the doping depth distributions for channeled implantations of B at energies ranging from 5 to 380 keV. All doping profiles were normalized to a dose of 1×10^{13} cm^{-2}. The actual dose ranged from 2×10^{12} to 2×10^{14} cm^{-2}. The influence of the energy on the shape of the resulting depth doping profiles is clearly illustrated. The profile is flat for the highest implantation energies and becomes more and more sharply peaked as the implantation energy is lowered. However, the decrease in B concentration at the maximum penetration depth is nearly constant with energy, roughly 23(2) decades/μm.

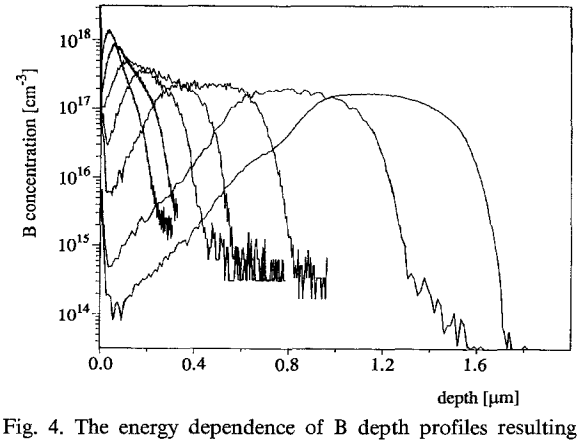

Fig. 4. The energy dependence of B depth profiles resulting from channeling implants at energies of 5, 10, 20, 40, 80, 200 and 380 keV. All doping depth profiles were normalized to a dose of 1×10^{13} cm^{-2}. The decay in B concentration at R_{max} is 23(2) decades/μm independent of energy.

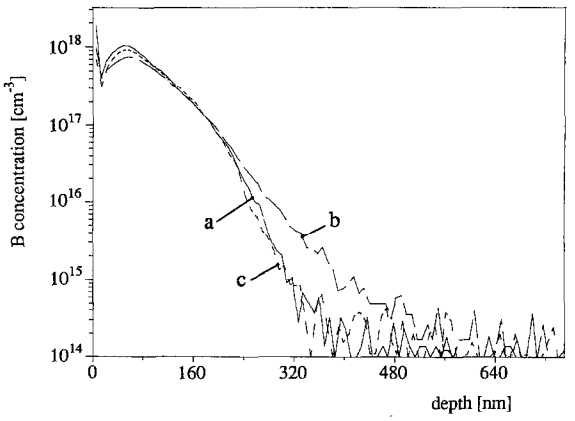

Fig. 5. Transient diffusion is illustrated for an implantation of 10 keV 1×10^{13} cm^{-2} B^+ ions in silicon. The as-implanted profile is referred to as (a) while the profile after RTA showing transient diffusion is referred to as (b). When the sample is post-amorphized with Ge^+ ions prior to annealing transient diffusion is avoided (c).

The effect of RTA anneals on the B profile is shown for a channeling implantation of 10 keV 1×10^{13} cm^{-2} in fig. 5. Transient diffusion of the B profile tail is observed after annealing at 900°C for 10 s. To prevent transient diffusion, samples were implanted with Si^+ or Ge^+ ions prior to annealing to form a 0.5 μm amorphous layer [13]. The B profile is completely incorporated in the amorphized layer. Annealing at 550°C for 5 h in vacuum followed by RTA at 900°C for 10 s results in

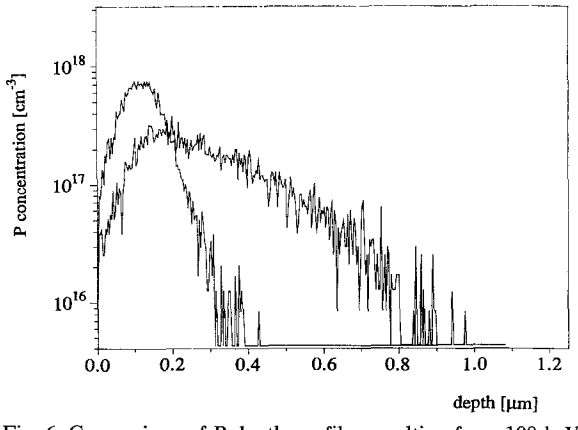

Fig. 6. Comparison of P depth profiles resulting from 100 keV 1×10^{13} cm^{-2} implantations under channeling and random conditions.

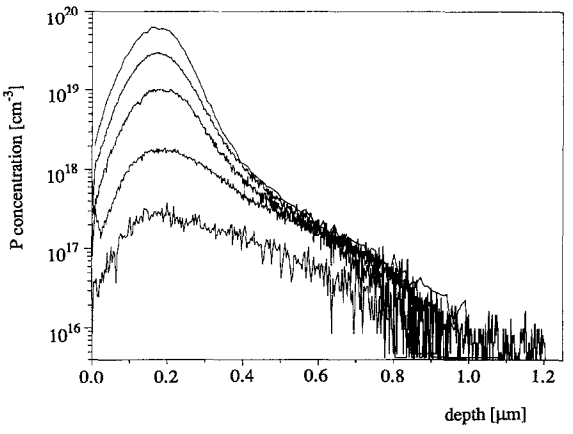

Fig. 7. Phosphorus depth profiles for implantations at 100 keV of 1×10^{13}, 5×10^{13}, 2×10^{14}, 5×10^{14} and 1×10^{15} cm^{-2}. Above 5×10^{13} cm^{-2} the number of P ions incorporated in the deep tail saturates and a strong increase in P concentration is observed around a depth of 190 nm.

the profile labeled (c). Clearly, post-amorphization eliminates the transient diffusion and a profile with a steep B falloff results.

3.2. Phosphorus implantations in Si(100)

Fig. 6 compares random and channeled implants of 100 keV 1×10^{13} cm^{-2} ^{31}P. A Gaussian profile peaked at 113 nm results for the random implant, in excellent agreement with TRIM [11] calculations. The channeling implantation leads to a doping profile extending to 0.8 μm.

The dose dependence of channeled implants of 100 keV ^{31}P are shown in fig. 7 for doses from 1×10^{13} to 1×10^{15} cm^{-2}. All profiles show the deep tail of well-channeled ions. The number of P ions in the deep tail saturates at a dose of 5×10^{13} cm^{-2} as the dechanneling probability increases with increasing damage in the silicon. Above 5×10^{13} cm^{-2} a strong increase in the P concentration is observed around a depth of 190 nm, which is more than 1.5 times the projected range of $R_p = 115$ nm for 100 keV P^+ ions under random condition.

The difference in damage produced by random and channeled implantations of 100 keV 2×10^{14} cm^{-2} P^+ ions has been studied using RBS in the (001) channeling configuration. Results are given in ref. [15]. The damage profile of the random implant peaks at a depth of 100 nm, which is consistent with a TRIM [11] calculation for 100 keV P^+ into amorphous silicon, while for the channeling implant the damage peaks at roughly 165 nm. The total damage level is significantly lower for the channeled implant as shown by quantitatively comparing the total number of displaced silicon atoms in both cases. Using the method of Chu et al. [14] the number of displaced atoms has been estimated to amount to 1.1×10^{17} cm^{-2} vs 3.4×10^{17} cm^{-2} for the channeling and random implantations, respectively. After annealing in vacuum at 900°C for 15 min we observe in both samples a band of dislocation loops at a depth of 110 and 160 nm for the random and channeling implants, respectively. The positions of the bands of dislocation loops correspond to the peak positions of the damage distributions. The concentration of dislocation loops is considerably lower for the channeled implant.

4. Conclusion

Extremely good uniformity has been achieved for channeling implantations in wafers up to 150 mm diameter. The combined effects of wafer orientation, beam parallelism and beam divergence result in angle deviations smaller than the critical angles for the ion species considered. For both B^+ and P^+ ions we observe a significant increase in the penetration depth. However, above a critical dose the difference between channeling and random implantations is no longer pronounced due to dechanneling by built-up disorder. The critical dose is 1×10^{14} cm^{-2} for 200 keV B^+ ions and 5×10^{13} cm^{-2} for 100 keV P^+ ions. Flat doping profiles up to 10^{17} cm^{-3} extending to a depth of 1–1.5 μm can easily be achieved by modest energy (100–200 keV) channeled implants of both B and P. Comparable profiles can be obtained only by multiple conventional (random) implantations at considerably higher energies. The strong reduction of nuclear interactions for channeled ions leads to reduced ion range straggling, and a consequently steep falloff in the B concentration on the substrate side of the doping profile. In addition, channeled implants result in a strong reduction in both implant damage and. the density of secondary defects formed during thermal annealing.

Acknowledgements

This work is part of the research program of the Stichting voor Fundamenteel Onderzoek der Materie and was made possible by financial support from the Nederlandse Organisatie voor Zuiver Wetenschappelijk Onderzoek and from Varian/Extrion (USA). We gratefully acknowledge J.S. Custer (FOM) for carefully reading the manuscript.

References

[1] H. Nishi, T. Inada, T. Sakurai, T. Kaneda, T. Hisatsugu and T. Furuya, J. Appl. Phys. 49 (1978) 60.

[2] D.W. Berrian, R.E. Kaim, J.W. Vanderpot and J.F.M. Westendorp, Nucl. Instr. and Meth. B37/38 (1989) 500.

[3] D.W. Berrian, R.E. Kaim and J.W. Vanderpot, Nucl. Instr. and Meth. B37/38 (1989) 518.
[4] J.D. Pollock, R.W. Milgate, R.F. McRay and R.E. Kaim, Nucl. Instr. and Meth. B37/38 (1989) 576.
[5] R. Kokaschke, R.E. Kaim, P.F.H.M. Van Der Meulen and J.F.M. Westendorp, IEEE Trans. Electron Devices 37 (1990) 1052.
[6] O.B. Firsov, Sov. Phys. JETP 36 (1959) 1076.
[7] E.V. Kornelsen, F. Brown, J.A. Davies, B. Domeij and G.R. Piercy, Phys. Rev. 136 (1964) A849.
[8] R.J. Schreutelkamp, F.W. Saris, J.F.M. Westendorp, R.E. Kaim, G.B. Odlum and K.T.F. Janssen, Mater. Sci. Eng. B2 (1989) 139.
[9] J.F.M. Westendorp, R.E. Kaim, J.W. Vanderpot, G.B. Odlum, R. Schreutelkamp and F.W. Saris, Solid State Techn. 31 (1988) 53.
[10] J.F.M. Westendorp, R.E. Kaim, G.B. Odlum, R. Schreutelkamp, F.W. Saris and K.T.F. Janssen, Nucl. Instr. and Meth. B37/38 (1989) 357.
[11] J.P. Biersack and L.G. Haggmark, Nucl. Instr. and Meth. 174 (1980) 257.
[12] W.K. Hofker, H.W. Werner, D.P. Oosthoek and H.A.M. de Grefte, Radiat. Eff. 17 (1973) 83.
[13] For details about the post-amorphization implants see R.J. Schreutelkamp, W.X. Lu, F.W. Saris, K.T.F. Janssen, J.J.M. Ottenheim, R.E. Kaim and J.F.M. Westendorp, in: Beam-Solid Interactions: Physical Phenomena, eds. P. Borgesen, J.A. Knapp and R.A. Zuhr (Mater. Res. Soc. Proc. 157, Boston, MA, 1989).
[14] W.K. Chu, J.W. Mayer and M.-A. Nicolet, Backscattering Spectrometry (Academic Press, New York, 1978).
[15] V. Raineri, R.J. Schreutelkamp, F.W. Saris, R.E. Kaim and K.T.F. Janssen, presented at IBMM 1990.